Martensitic fcc-to-hcp Transformation Observed in Xenon at High Pressure

H. Cynn,[1] C. S. Yoo,[1] B. Baer,[1] V. Iota-Herbei,[1] A. K. McMahan,[1] M. Nicol,[2] and S. Carlson[3]

[1]*H-Division, Physics and Advanced Technology Directorate, Lawrence Livermore National Laboratory, University of California, Livermore, California 94550*

[2]*High Pressure Science and Engineering Center, University of Nevada–Las Vegas, Las Vegas, Nevada 89154-4002*

[3]*European Synchrotron Radiation Facility, Grenoble, France*

(Received 18 August 2000)

Angle-resolved x-ray diffraction patterns of Xe to 127 GPa indicate that the fcc-to-hcp transition occurs martensitically between 3 and 70 GPa in diamond-anvil cells without an intermediate phase. These data also reveal that the transition occurs by the introduction of stacking disorder in the fcc lattice at low pressure, which grows into hcp domains with increasing pressure. The small energy difference between the hcp and the fcc structures may allow the two phases to coexist over a wide pressure range. Evidence of similar stacking disorder and incipient growth of an hcp phase are also observed in solid Kr.

DOI: 10.1103/PhysRevLett.86.4552 PACS numbers: 61.50.Ks, 61.72.Hh, 61.72.Nn, 64.30.+t

Electronic transitions lie at the heart of many high-pressure phenomena including structural stability and metallization [1]. Such changes in the underlying electronic structure drive concomitant sequences of structural phase transitions, which have received intense recent interest for the alkali and alkaline earth metals [2]. There are other well-known examples of transitions showing structural systematics among the same group elements and compounds, e.g., the fcc-sc transitions of the alkali halides and alkaline earth oxides. In this respect, the rare-gas solids are unusual. He and Xe transform from fcc structures to hcp structures at high pressures; but corresponding transitions have not been reported for Ne, Ar, or Kr [3]. For Xe and other heavy rare-gas solids, it has been suggested [4] that hybridization between the s, p valence and the approaching d bands stabilizes the hcp structure at pressures below that of metallization (130–150 GPa for Xe) [5,6]. However, the manner and sequence by which xenon evolves from its ambient fcc phase to this high-pressure hcp phase and the systematics for other rare-gas solids remain unclear. Previous diffraction studies variously suggest a separate phase intervenes between the fcc phase and the hcp phase which appears at 75 GPa [7], stacking faults have a role in the transition to this middle phase [8], or that the direct fcc to hcp transition occurs at 21 GPa and is kinetically sluggish [9]. Clearly, the crystal structure data for xenon at high pressure need further elaboration to determine the boundary and mechanism of the structural evolution from fcc to hcp. Here we report angle-dispersive x-ray diffraction (ADX) evidence of the importance of stacking disorder and growth of domains of hcp Xe coexisting with fcc Xe over a wide range of high pressures at ambient and high temperatures that provide a better understanding of the mechanism of the fcc-to-hcp transformation of Xe. For Kr, we also find evidence of a similar coexistence of the ambient fcc and high-pressure hcp phases, which has not previously been observed [3].

To better characterize the crystal structures of Xe, especially the transition from the fcc and the hcp phases, we made high-resolution ADX measurements at the Stanford Synchrotron Radiation Laboratory (SSRL, 20 keV, 30-μm beam diameter at the sample) and at ID30 of the European Synchrotron Radiation Facility (ESRF, 22 keV, $\sim$8-μm beam diameter). The x-ray diffraction patterns were collected with image plates placed within 20–30 cm from the sample. The x-ray measurements below 80 GPa were done at the SSRL by using 300 μm diamond culets and at higher pressures at the ESRF by using 100 μm flats beveled from 300 μm culets. Rubies were used to measure pressures. In order to understand effects of strain and the fcc/hcp phase boundary suggested at 21 GPa [9], one sample at 29 GPa was laser heated indirectly by irradiating the ruby grains ($<$3 μm in diameter) using a Nd:YAG laser. Temperatures were not measured during heating. Some samples were also heated externally for *in situ* high-temperature ADX measurements; in these experiments, temperatures were measured by using an alumel-chromel thermocouple in contact with the diamond anvil and gasket. To explore the systematics in the fcc-to-hcp phase transition of rare-gas solids, a few similar ADX patterns were collected for Kr.

Figure 1 shows the angle-resolved x-ray diffraction patterns of Xe to 127 GPa at ambient temperature. At 3.7 GPa, thirteen peaks were detected to $2\Theta = 40°$. The peaks were indexed with good intensity matches to an ideal fcc structure, suggesting that effects of preferred orientation are relatively small. Significantly, two extra features are evident in the 3.7-GPa pattern in Fig. 1: a peak near $2\Theta = 11°$ and the raised background and the asymmetry of the fcc (111) peak near $2\Theta = 12°$. These extra features grow in intensity at higher pressures. In patterns at 29 GPa (before laser heating) and at 25 GPa (quenched after laser heating), the first extra feature is a peak as intense as the fcc (111), the second peak in these patterns which also corresponds to the hcp (002) peak. The raised background also develops into a broad peak, the third peak of these patterns. In contrast to the growth of the first and third peaks, the intensity of fcc (200)

 0031-9007/01/86(20)/4552(4)$15.00

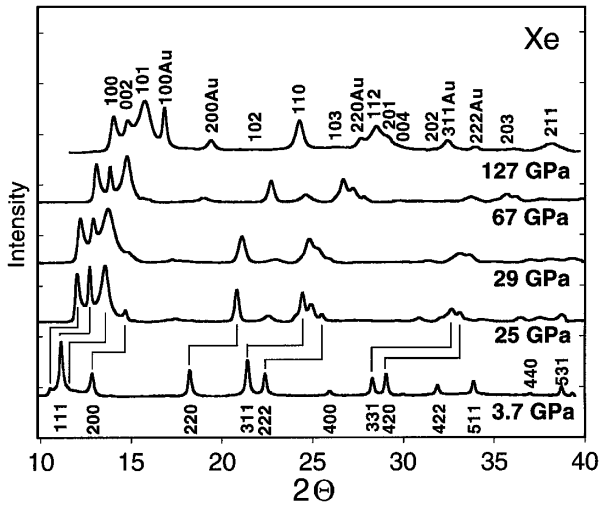

FIG. 1. Angle-resolved x-ray diffraction patterns of solid Xe at high pressures. The 25-GPa pattern was measured after laser heating the sample at 29 GPa. Miller indices for the fcc and hcp structures are also provided; the same diffraction lines are also correlated by thin lines for clarity. Note that two weak features adjacent to the fcc (111) peak at 3.7 GPa become the (100) and (101) reflections of hcp, suggesting that stacking faults occur along the fcc [111] direction.

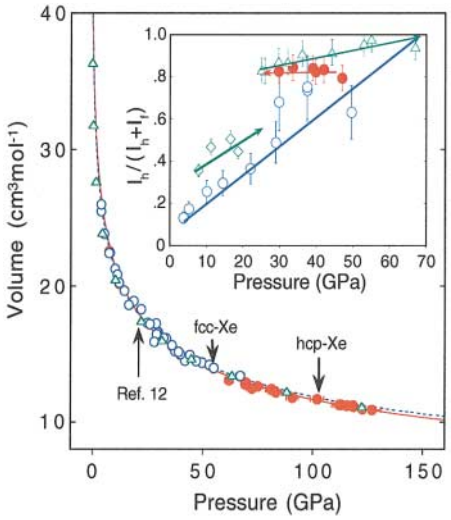

FIG. 2 (color). Volume compression data of fcc (○) and hcp (●) Xe to 127 GPa, together with the Birch-Murnaghan fits shown as dotted and solid curves, respectively. The augmented-plane-wave computations (see Ref. [11]) are also shown for comparison. The inset illustrates the relative amounts of hcp to fcc Xe at high pressures, clearly showing completion of the fcc-to-hcp transition at 70(±5) GPa regardless of the P-T history of samples. I_f and I_h are intensities of fcc (200) and hcp (100) reflections, respectively. It contains the data during compression (○ and ◇), decompression (●), and compression of the laser-quenched sample (△). The arrows in the inset represent the linear fits of the data.

decreases continuously with increasing pressure. Two further differences are evident between the patterns collected before (29 GPa) and after (25 GPa) heating. First, the 4-GPa reduction of pressure shifts all peaks to lower 2Θ angles. Second, after heating and quenching, the peaks are sharper and better resolved than before heating.

After further compression to 67 GPa, the fcc (200) is very weak; and peaks at around $2\Theta = 18$ and 24° appear to have grown in intensity. These two broad peaks, indexed as the hcp (102) and (103), start to develop between 14 and 25 GPa. On the other hand, the diffraction pattern at 127 GPa consists of twelve peaks for hcp Xe and five for gold used for the pressure standard [10]. The intensities of the hcp (102) and (103) peaks in this pattern are weaker and broader than those measured at 67 GPa. This pattern is similar, although less well-resolved, to a hcp Xe pattern at 160 GPa in Ref. [11]. The differences may reflect different grain sizes of these polycrystalline samples resulting from different compression histories.

As shown in Fig. 1, the (111), (220), (311), and (222) reflections of the fcc phase become the (002), (110), (112), and (004) reflections of the hcp phase, respectively. These correspondences are expected from disorder to stacking of close-packed atomic layers. Peaks that disappear are inherent to the fcc structure, its (200) and (400). The new peaks are inherent for the hcp structure, its (100), (101), (102), (103), (200), (201), (202), and (203). The widths of the peaks imply that the dimensions of individual domains of fcc or hcp order are at least many nanometers.

Figure 2 compares equations of state (EOS) for the fcc and hcp Xe phases with data from theory [12]. Volumes for fcc Xe were obtained to 70 GPa; at higher pressures, the fcc (200) disappears. Volumes for hcp Xe were obtained from 7 to 127 GPa. To refine the cell parameters, the diffraction patterns were fit by a set of Lorentzian profiles and a smooth background; the parameters were computed from the d spacings using a least-squares routine. The inset of Fig. 2 shows the relative fractions of hcp Xe in several samples, as estimated from relative intensities of the hcp (100) and fcc (200) reflections (each of which relates to only one structure). The data clearly show strong dependence of the fcc/hcp ratio on the pressure-temperature path of samples. For example, a sample directly compressed to 70 GPa (○) shows a linear increase in the amount of hcp crystallites. However, during decompression of a sample from 50 to 29 GPa (●), the fcc/hcp ratio remains the same. It is apparent from other samples (◇ and △) that the ratio also depends on the initial condition of the sample. These observations demonstrate a profound hysteresis of the fcc/hcp transition below 70 GPa. Nevertheless, it is apparent that the hcp-fcc transition is completed at 70(±5) GPa at ambient temperature, regardless of the thermodynamic path of samples.

Fits of these volume data using third-order Birch-Murnaghan equations yield values for the bulk modulus B_0 and its pressure derivative B_0' of 3.6(±0.5) GPa and 5.5(±0.4) for fcc Xe and 4.3(±0.3) GPa and 4.9(±0.1) for hcp Xe. In these fits, V_0 was constrained to the value, 37.97 cm^3/mol, obtained by extrapolating our high-pressure volume data to ambient conditions for both

fcc Xe and hcp Xe. Although this constrained volume at ambient conditions is substantially larger than the volume at 4 K, 34.7 cm^3/mol, used in the previous EOS fits [5,13], it is within 1.5% of the molar volume, 38.49 cm^3/mol of solid Xe near its melting point at ambient pressure [14]. The 0-K isotherm [12] predicted by augmented-plane-wave calculations appears to be in good agreement with our 300-K isotherm.

In several systems, disorder in the stacking of atomic layers develops during martensitic transformations. In cobalt, this occurs during martensitic transitions between fcc and hcp phases upon cooling at ambient pressure [15] and from hcp to fcc during compression at high pressure [16]. Figure 3(a) shows anomalous streaks and diffuse spots between the fcc (111) and fcc (200) x-ray diffraction rings as well as near the hcp (100) and fcc (111) rings in the x-ray diffraction image of xenon at 3.7 GPa (see inset 1). A similar pattern indicating the existence of hcp peaks was obtained from the ADX images of Kr near 2 GPa [Fig. 3(b)]. The streaks of the hcp (100) reflection in Kr emanate as (nonradial) lines (see inset 3), and the hcp (101) reflections appear as diffuse spots (see inset 4) and streaks (see inset 2) between fcc (111) and fcc (200) reflections. Similar streaks and integrated x-ray diffraction features are observed in the martensitic fcc to hcp transition in Cu-Ge alloys, where they are also attributed to stacking disorder [17]. Electron micrographs of Xe at 20 K show stacking faults as narrowly spaced parallel lines, and x-ray diffraction patterns show long streaks and diffuse spots [18].

The peaks indicative of a disordered hcp structure of xenon are apparent from the (100) and (101) reflections of hcp Xe in the 2D image measured at 14 GPa and at high temperature and its integrated 1D angle-resolved x-ray diffraction pattern [Fig. 4(a)]. The features from disordered hcp Xe disappear and the (111) and (200) peaks of fcc Xe become sharper during decompression [Fig. 4(b)]. This stacking-disorder-free x-ray diffraction pattern of fcc Xe clearly confirms that formation of disordered hcp Xe, evolution to ordered hcp Xe, and complete disappearance of fcc Xe at high pressures is not impurity induced.

In summary, a martensitic transformation of Xe is initially detected by the appearance of features attributed to stacking disorder along the fcc [111] close-packing direction and which evolves into an hcp structure at higher pressures. That this fcc-to-hcp transformation occurs over a wide range of pressures differs from previous interpretations that suggest an intermediate phase, Xe (II) [7,8]. The transition appears to be continuous in Ubbelohde's classification [19] because the local stress tensor in these DAC samples is neither diagonal in the pressure nor well-controlled. Quenching after laser melting did not change the extent of stacking disorder.

Both deformation faults observed by streaks and diffuse scattering and the insensitivity of phase stability to laser heating support the interpretation in terms of a martensitic change between fcc and hcp phases of nearly equal free energies over a broad range of applied "pressures." The complete disappearance of the fcc (200) peak suggests that the boundary between the fcc and hcp phases may be as high as 70(±5) GPa. The evolution of domains of hcp Xe from the fcc material with increasing pressure results from a complex interplay of the introduction of stacking

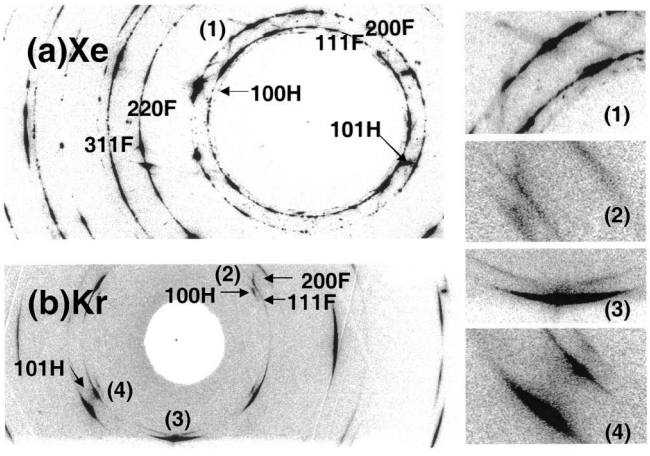

FIG. 3. Debye-Scherrer diffraction rings as recorded on image plates of (a) Xe at 3.7 GPa and (b) Kr at 2 GPa, showing the evidence for diffuse scattering near the (111) and (200) rings of the fcc structures. *F* and *H* are for fcc and hcp patterns, respectively. Insets of enlarged images are labeled for visual help.

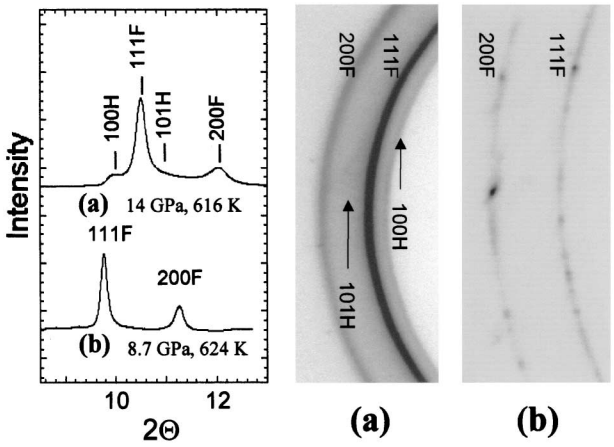

FIG. 4. *In situ* angle-resolved x-ray diffraction patterns of Xe near 620 K and high pressures: (a) at 14 GPa and (b) 8.7 GPa after decompression from (a). These patterns show the transition of Xe from an fcc/hcp mixture at 14 GPa to pure fcc at 8.7 GPa at 616 K. *F* and *H* are for fcc and hcp patterns, respectively. The raised background in the integrated diffraction pattern and darker background intensity from the x-ray image (a) as shown by arrows provide evidence for (101)*H* scattering. Further support for this interpretation comes from deconvolution of the integrated intensity of the 14-GPa pattern between 9 and 13.5° in 2Θ. When the pattern is fit by three intermediate Lorentzian profile-shaped functions, the residual error is 14%; the residual error was reduced to less than 1% by adding a fourth intermediate Lorentzian profile at approximately 13°.

disorder, growth of new domains, and relaxation of local stress fields as the applied pressure increases. Evidence for a similar transformation by intergrowth of hcp domains within an fcc lattice in krypton is shown in Fig. 3(b), suggesting that corresponding high-pressure hcp phases may be systematic among the heavy rare-gas solids. The present work and earlier theoretical studies raise the possibility that the electronic s, p to d transition, which metallizes xenon and should metallize krypton, also drives the uncommon continuous transitions from fcc and hcp seen here in these solids, accomplished via the successive introduction of more and more hexagonal stacking faults in the original fcc material [20].

We thank K. Visbeck, H. Reichman, and A. Treat for their assistance at SSRL and ESRF. This work was performed under the auspices of the U.S.-DOE by UC-LLNL under Contract No. W-7405-Eng-48 and by the UNLV under Cooperative Agreement DE-FC08-98NV13410.

[1] R. J. Hemley and N. W. Ashcroft, Phys. Today **51**, No. 8, 26 (1998).

[2] U. Schwarz, A. Grzechnik, K. Syassen, I. Loa, and M. Hanfland, Phys. Rev. Lett. **83**, 4085 (1999); R. J. Nelmes, D. R. Allan, M. I. McMahon, and S. A. Belmonte, Phys. Rev. Lett. **83**, 4081 (1999).

[3] D. A. Young, *Phase Diagrams of the Elements* (University of California Press, Oxford, 1991). See Fig. 12.12 in this reference for structural data of Xe and Kr. Kr is stable as fcc to near 100 GPa according to the previous studies. No stacking disorder or coexisting hcp domains have previously been reported for Kr at high pressures.

[4] A. K. McMahan, Phys. Rev. B **33**, 5344 (1986). Results for Xe are similar, with the hcp energy $\sim$1.6 mRy/atom lower than fcc at 70 GPa, and dropping rapidly with larger pressures.

[5] R. Reichlin *et al.,* Phys. Rev. Lett. **62**, 669 (1989); K. A. Goettel *et al.,* Phys. Rev. Lett. **62**, 665 (1989).

[6] M. I. Eremets, E. A. Gregoryanz, V. V. Struzhkin, H. Mao, and R. J. Hemley, Phys. Rev. Lett. **85**, 2797 (2000).

[7] A. P. Jephcoat *et al.,* Phys. Rev. Lett. **59**, 2670 (1987).

[8] A. P. Jephcoat *et al.,* in *Proceedings of the International Conference—AIRAPT-16 and HPCJ-38—on High Pressure Science and Technology* (AIRAPT, Kyoto, Japan, 1997).

[9] W. A. Caldwell *et al.,* Science **277**, 930 (1997).

[10] D. L. Heinz and R. Jeanloz, J. Appl. Phys. **55**, 885 (1984).

[11] K. Brister, Rev. Sci. Instrum. **68**, 1629 (1997).

[12] M. Ross and A. K. McMahan, Phys. Rev. B **21**, 1658 (1980).

[13] K. Syassen and W. B. McMahan, Phys. Rev. B **18**, 5826 (1978); A. Jephcoat, Nature (London) **393**, 355 (1998).

[14] M. S. Anderson and C. A. Swenson, J. Phys. Chem. Solids **36**, 145 (1975).

[15] F. Frey and H. Boysen, Acta. Crystallogr. Sect. A **37**, 819 (1981).

[16] C. S. Yoo *et al.,* Phys. Rev. Lett. **84**, 4132 (2000).

[17] P. S. Kotval and R. W. K. Honeycombe, Acta Metall. **16**, 597 (1968). See Figs. 3–5 and 18 in this reference for a visual comparison of the similar streaks and diffuse spots in the diffraction images.

[18] R. Bullough, H. R. Glyde, and J. A. Venables, Phys. Rev. Lett. **17**, 249 (1966).

[19] A. R. Ubbelohde, Quart. Rev. (London) **11**, 246 (1968).

[20] It would be interesting, for example, if theoretical calculations could connect the electronic transition to competing interlayer interactions shown in Ising models to lead to such stacking fault structures [see, e.g., G. D. Price and J. Yeomans, Acta. Crystallogr. Sect. B **40**, 448 (1984), and references therein.]